https://doi.org/10.52973/rcfcv-e34380 Revista Científica, FCV-LUZ / Vol. XXXIV, rcfcv-e34380

Pathological Investigation of Double–Stranded DNA Breaks and DNA Oxidation in Natural Infection with *Mycobacterium avium* subspecies *paratuberculosis* in Goats

Investigación patológica de las roturas de DNA de doble cadena y la oxidación del DNA en la infección natural por *Mycobacterium avium* subespecie *paratuberculosis* en cabras

***Muhammet Bahaeddin Dörtbudak*[1]*, *Merve Öztürk*[2]**

[1]*Harran University, Faculty of Veterinary Medicine, Department of Pathology. Sanliurfa, Türkiye.*
[2]*Necmettin Erbakan University, Faculty of Veterinary Medicine, Department of Internal Medicine. Konya, Türkiye.*
**Corresponding author: mbdortbudak@gmail.com*

ABSTRACT

Paratuberculosis, created by *Mycobacterium avium* subspecies *paratuberculosis* (MAP), manifests as a chronic affliction marked by persistent diarrhoea and granulomatous enteritis, pervasive in both domestic and global wild ruminants. In this investigation, DNA disruption in lesioned tissues of goat as natural infecte with MAP was pathologically assessed. Accordingly, goats manifesting symptoms suggestive to paratuberculosis, including pronounced emaciation and continual episodic diarrhoea, were subjected to an ELISA diagnostic procedure to ascertain the presence of MAP. This diagnostic approach confirmed the presence of the infectious agent in 20 patients. These patients were subsequently euthanized, and tissue samples from intestinal and regional lenf nods. It were subjected to Hematoxylin and Eosin (HE) staining for histopathological investigatıon, Ziehl Neelsen (ZN) staining to identify acid-fast mycobacteria, γ-H2AX to discern disruptions in double stranded DNA, and 8-Ohdg to detect DNA oxidation by immunohistochemical (IHC) method. Gross anatomical observation serous adipose atrophy, augmented dimensions of mesenterial lymphatic nodes, mucosal hypertrophy and non-retractable mucosal undulations. Histological assessment highlighted epithelial cellular degeneration, an abundance of epithelioid macrophages, lymphocytes, plasmocytes, infiltrating in mucosa. Acid-fast entities, discernible through ZN staining, appeared as luminescent red conglomerates in intestinal and mesenterial tissue. The immunohistochemical analyses evinced positive results for both γ-H2AX and 8-Ohdg across all sampled tissues. Intriguingly, this investigation presented the inaugural global evidence of γ-H2AX and 8-Ohdg expression in a natural MAP infection, demonstrating that this pathological agent precipitates DNA degradation and oxidation, thereby augmenting comprehension of the disease's pathogenesis.

Key words: Goat; MAP; paratuberculosis; γ-H2AX; 8-Ohdg

RESUMEN

La paratuberculosis, provocada por *Mycobacterium avium* subespecie *paratuberculosis* (MAP), se manifiesta como una afección crónica marcada por diarrea persistente y enteritis granulomatosa, generalizada en rumiantes domésticos y salvajes del mundo. En esta investigación se evaluó patológicamente la alteración del DNA en tejidos lesionados de cabra infectada naturalmente por MAP. En consecuencia, las cabras que manifestaban síntomas sugestivos de paratuberculosis, incluida emaciación pronunciada y diarrea episódica continua, se sometieron a un procedimiento de diagnóstico ELISA para determinar la presencia de MAP. Este procedimiento de diagnóstico confirmó la presencia del agente infección en 20 pacientes. A continuación, se practicó la eutanasia a estos pacientes y se tomaron muestras de tejido de los ganglios linfáticos intestinales y regionales. Se sometieron a tinción de Hematoxilina y Eosina (HE) para la investigación histopatológica, tinción de Ziehl Neelsen (ZN) para identificar micobacterias acidorresistentes, γ-H2AX para discernir alteraciones en el DNA de doble cadena y 8-Ohdg para detectar la oxidación del DNA mediante el método inmunohistoquímico (IHQ). Observación anatómica macroscópica atrofia adiposa serosa, aumento de las dimensiones de los ganglios linfáticos mesenteriales, hipertrofia mucosa y ondulaciones mucosas no retráctiles. La evaluación histológica destacó degeneración celular epitelial, abundancia de macrófagos epitelioides, linfocitos, plasmocitos, infiltrados en la mucosa. Las entidades ácido-alcohol resistentes, distinguibles mediante tinción de ZN, aparecían como conglomerados rojos luminiscentes en el tejido intestinal y mesenterial. Los análisis inmunohistoquímicos mostraron resultados positivos tanto para γ-H2AX como para 8-Ohdg en todos los tejidos muestreados. Curiosamente, esta investigación presentó la evidencia global inaugural de la expresión de γ-H2AX y 8-Ohdg en una infección natural por MAP, demostrando que este agente patológico precipita la degradación y oxidación del DNA, con lo que aumenta la comprensión de la patogénesis de la enfermedad.

Palabras clave: Cabra; MAP; paratuberculosis; γ-H2AX; 8-Ohdg

Received: 17/01/2024 Accepted: 18/03/2024 Published: 26/06/2024

INTRODUCTION

Paratuberculosis manifests as chronic diarrhea and cachexia in ruminants. Globally prevalent, this disease inflicts substantial economic impacts through reductions in milk output, live weight, and can even lead to the death of the animals. There's evidence to suggest a link between this disease in both wild and domestic ruminants and Crohn's disease in humans. However, it's currently not identified as a zoonosis. Furthermore, the discovery of the disease-causing agents in raw milk from affected animals poses food safety concerns [1, 2, 3].

Mycobacterium avium subspecies *paratuberculosis* (MAP) is identified as the etiological agent of paratuberculosis. This bacterium is acid-resistant, gram-positive, devoid of spores, rod-shaped, and can persist within macrophages. The disease exhibits a high prevalence but low fatality rate. Transmission is commonly through water and food sources contaminated with infectious secretions, including direct contact, faeces, urine, and saliva. Reports also indicate possible intrauterine transmission to the offspring. Although young ruminants are highly vulnerable, manifestations aren't evident in animals younger than 2 years, attributed to the disease's extended incubation period [4, 5]. The primary site of infection after oral intake is the gastrointestinal system, predominantly affecting the terminal sections of the small intestine and adjacent lymph nodes. The most evident clinical manifestation is chronic diarrhea, frequently accompanied by dehydration, cachexia, depression, submandibular swelling, and diminished milk production. In deceased animals, granulomatous enterocolitis and localized lymphadenitis are commonly present. On a histopathological level, infiltration of lymphoplasmacytic cells, predominantly epithelioid histiocytes, is noticeable. While no conclusive treatment exists and its zoonotic nature remains unverified, a general recommendation is the culling of infected animals, even though reporting the disease isn't mandatory [3, 6, 7, 8].

Recent research underscores the impact of pathogenic agents on cellular damage, with DNA damage being a fundamental mechanism of such injury. Two pivotal biomarkers for DNA damage are γ-H2AX and 8-OhdG. The γ-H2AX protein, a member of the H2A family, is integral to the DNA repair process. Phosphorylation of histone proteins initiates the emergence of γ-H2AX, which facilitates the primary assembly of DNA repair proteins at the site of double-strand breaks. Consequently, γ-H2AX is currently recognized as a vital indicator of DNA breakages in scientific investigations [9, 10]. On the other hand, 8-OHdG, another DNA damage biomarker, is indicative of DNA oxidation. It emerges from the oxidation of the 8th carbon atom of the guanine base in DNA by free radicals and is acknowledged as a marker for DNA damage attributed to oxidative stress [11, 12].

This research study aimed to probe the deleterious impact of pathogens on DNA to shed light on the pathogenesis of paratuberculosis, a significant health concern for domestic ruminants globally. To achieve this, the study assessed the presence of γ-H2AX and 8-OhdG expressions, current biomarkers, in the affected tissues of naturally infected animals, thereby ascertaining DNA damage.

MATERIALS AND METHODS

Animal Material

In this study, the materials of the study conducted with the ethical approval of Bıngol University Animal Experiments Local Ethics Committee (B.Ü. AELEC 2023/02-02/13) were used. The subjects of the research were 20 female hair goats *(Capra hircus),* aged between 2 to 5 years. Blood samples were collected from mature animals displaying symptoms suggestive of paratuberculosis, such as consistent intermittent diarrhea, pronounced emaciation, and diminished productivity. The presence of the disease was diagnosed using the ELISA test. Subsequent to the testing, all 20 animals suspected of having paratuberculosis were confirmed to be infected with MAP. Given the lack of an effective treatment and to thwart environmental contamination, the affected animals were euthanized. Postmortem examinations of these animals displayed signs of paratuberculosis, particularly in the intestines and mesenteric lymph nodes. For further histopathological and immunopathological evaluations, samples from the affected tissues were secured and preserved in a 10% buffered formalin solution.

ELISA Test

Blood sera from suspected infected animals were analyzed for MAP antibodies using a commercial ELISA kit (Paracheck 2, no.63325, Prionics AG, Zurich, Switzerland) to detect the presence of infection antibodies. The testing procedure adhered strictly to the manufacturer's prescribed protocol. Post-reaction, the optical density (OD) of each well was measured using an ELISA reader (Rayto, RT-2100C, China) fitted with a 450 nm filter.

Tissue Processing

Tissues preserved in a 10% buffered formalin solution were rinsed in running tap water before undergoing rutine tissue processing. From the processed tissue samples, paraffin blocks were produced. Sections measuring 5 µm in thickness were then cut from each block onto both normal and polylysine-coated slides using a rotary microtome (Leica, RM2135, Germany).

Histopathological Examination

Tissue sections placed on conventional slides were oven-dried for an hour, followed by deparaffinization and rehydration. To observing in tissue histopathological changes and acid-resistant microorganisms, HE and ZN staining techniques were employed, respectively [13]. After staining, each tissue section was covered with a coverslip using a drop of Entellan™ and subsequently observed under a light microscope (Leica, DM2500, Germany).

Immunohistochemical Staining

Tissue sections placed on polylysine slides underwent oven drying for an hour before deparaffinization and subsequent rehydration through a xylol-alcohol series. Endogenous peroxidase activity was quenched by immersing the tissues in 3% H_2O_2 for 10 min. Following a PBS wash, antigen retrieval was achieved by boiling the tissues three times in a retrieval solution. Another PBS wash was followed by outlining the tissue sections with a PAP pen and then blocking non-specific binding sites using Ultra V Block for 20 minutes. The primary antibodies, γ-H2AX (no. NB100-2280SS, NovusBio, USA) and 8-Ohdg (no. sc66036, Santa Cruz, USA), were diluted at a 1/100 ratio and then incubated at +4°C overnight. After a PBS wash, biotinylated secondary antibody was applied to the tissues, followed by a 20 min incubation. Following another PBS wash, streptavidin-peroxidase was added for an additional 20 min. Upon the final PBS wash, 3,3' -Diaminobenzidine (DAB) chromogen was introduced to the sections to visualize the antigen-antibody interaction. After counterstaining with Mayer Haematoxylin, the sections, now covered with coverslips, were analyzed under a light microscope [13].

RESULTS AND DISCUSSIONS

ELISA Test

ELISA test was performed on the blood sera of 20 goats with suspected MAP infection in clinical findings. According to the arithmetic mean (S/P(+)≥ 0.50) calculated from the optical densities of the tested serum samples, 20 goat sera with suspected infection in the study were positive for MAP infection.

Macroscopic Findings

Upon postmortem examination of infected goats that were euthanized and sent to slaughter, notable lesions were detected in the intestine and its adjacent lymph nodes. In the abdominal cavities, there was a presence of about 2–3 L of either serous or serofibrinous exudate. The mesentery, omentum, and subperitoneal fatty tissue exhibited signs of atrophy and were substituted by a widespread yellowish gelatinous edema. The serosa of the intestine appeared cloudy due to pervasive edema. Furthermore, mucosal thickening and undulating folds, which remained rigid even when tugged, were evident. The intestinal chambers contained watery content. While the lesions permeated almost all segments of the intestine, they were predominantly located in the ileum, jejunum, and to some extent in the proximal section of the cecum. The lymphatic vessels appeared cord–like due to thickening, and the mesenteric lymph nodes were markedly enlarged. Cross–sections of the edematous lymph nodes revealed them to be engorged, making it challenging to discern between the cortex and medulla. (FIG.1. A–B)

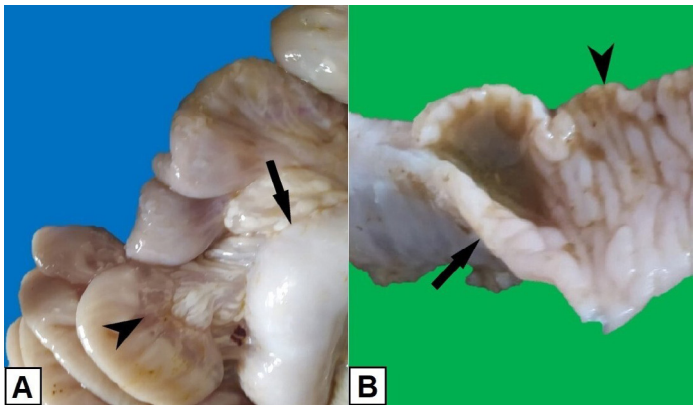

FIGURE 1. Gross pathology. A; Serous fat atrophy in the mesenterium (arrowhead) and severe edema in the mesenterial lymph node (arrow). B; Thickening (arrow) and transverse folds (arrowhead) of the intestinal mucosa

Histopathological Findings

Histopathological evaluations indicated pervasive proliferative inflammation encompassing nearly all intestinal layers, with pronounced effects in the jejunum and ileum. Noteworthy morphological alterations included villi atrophy, fusion, and flattening, coupled with substantial degeneration and shedding of enterocytes. The mucosal lamina propria displayed edema, intensive inflammatory cell infiltrations, and marked expansion, partly attributed to increased fibrous connective tissue. Predominantly, the inflammatory cell population was composed of mononuclear leukocytes, including macrophages, lymphocytes, and plasmocytes, complemented by a presence of neutrophils and eosinophils. Notably, collections of focal epithelioid macrophages were commonly identified, while the presence of giant cells was infrequent. The described epithelioid cells typically exhibited a round to oval morphology with peripherally positioned euchromatic nuclei and cytoplasm that was either eosinophilic or foamy. The villous lacteals and Lieberkühn crypts displayed notable cystic dilatation and desquamation (FIG. 2. A–B).

In the submucosa, inflammatory manifestations mirrored those in the lamina propria. The lymphoid structures within the submucosa displayed hyperplasia and perilymphangitis. Despite an absence of detectable lesions in the muscularis layer, the serosa exhibited edema, subtle leukocyte infiltrations, and lymphangitis (FIG. 2. C).

In examining the mesenteric lymph nodes, a notable enlargement and fluid retention were observed in nearly all sinuses. The cortex demonstrated generalized lymphoid hyperplasia, and microgranulomas consisting of epithelioid macrophages were evident within the paracortical region and subcapsular sinuses (FIG. 2. D). ZN staining

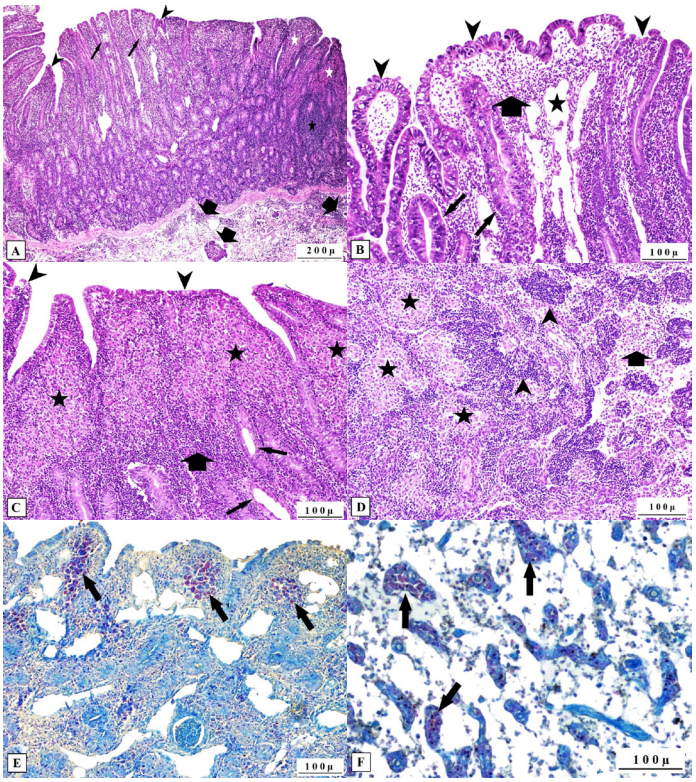

FIGURE 2. Histopatology. A; Atrophy and fusion of villi (arrowheads), inflammatory cell infiltrations in the lamina propria (thin arrows), epithelioid histiocyte aggregations (white stars), lymphoid hyperplasia (black stars), inflammatory cell infiltration and lymphangitis in the submucosa (thick arrows), HE, 4×. B; Severe degeneration and desumation of enterocytes (arrowheads), edema and inflammatory cell infiltration in villous lamina propria (thick arrow), cystic dilatation in crypt glands and degeneration of epithelial cells (thin arrows), enlargement of villous lacteals (star), HE, 10×. C; Degeneration in enterocytes (arrowheads), epithelioid histiocyte aggregation in lamina propria (stars), mononuclear cell infiltration in lamina propria (thick arrow), cystic dilation in crypt glands (thin arrows), HE, 10×. D; Epithelioid cell granulomas (stars), edema and inflammatory cell infiltrates (thick arrow), lymphoid hyperplasia (arrowheads), HE, 10× in the mesenterial lymph node. E; Areas showing acid–fast mycobacteria suggestive of Mycobacterium avium subspecies paratuberculosis (arrows) in the lamina propria, ZN, 10×. F; Areas showing acid–fast mycobacteria suggestive of Mycobacterium avium subspecies paratuberculosis (arrows) in mesenterial lymph node ZN, 10×

showcased a plethora of vivid red acid-fast entities, primarily internalized by epithelioid cells within the villous lamina propria or in external clusters. Epithelioid macrophages, and extracelluler areas in mediastinal lenf nodes, acid-fast mycobacteria suggestive of Mycobacterium avium subspecies paratuberculosis as confirmed, albeit in reduced numbers (FIG. 2. E-F).

Immunohistochemical Findings

Immunohistochemical analysis using γ-H2AX revealed immunoreactivity within the degenerated mucosal epithelium, lamina propria-infiltrating leukocytes, crypt epithelial cells, and in the nuclei of most epithelioid macrophages. Additionally, intranuclear staining of epithelioid macrophages was evident in the mediastinal lymph nodes, particularly in areas with lymphoid hyperplasia (FIG 3. A-C). When employing 8-Ohdg for immunohistochemical staining, intranuclear staining was identified in leukocytes and epithelioid cells within the lamina propria, submucosa, and mediastinal lymph nodes. Furthermore, degenerated enterocytes displayed immunoreactivity for 8-Ohdg (FIG. 3. D-F).

Paratuberculosis, stemming from MAP, represents a significant health concern for domestic ruminants, inflicting substantial economic repercussions. This ailment, prevalent across various global regions for an extended period, persists in its widespread nature, with afflicted animals typically exhibiting chronic diarrhea and deteriorating physical conditions [3, 14]. The present study's subjects, based on their clinical histories and symptoms, predominantly displayed intermittent, persistent diarrhea coupled with pronounced emaciation, mirroring findings from prior natural and experimental infection research.

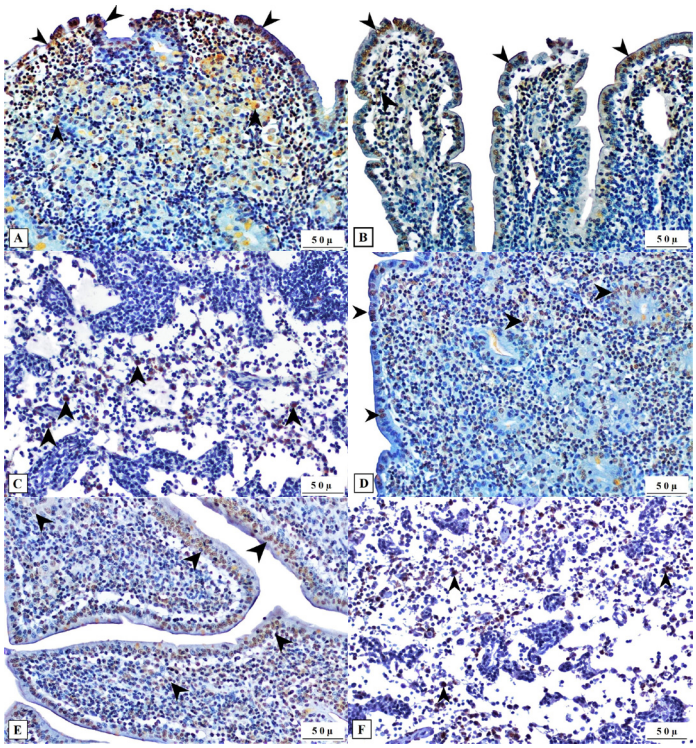

FIGURE 3. Immunopathology; A; Expression of γ-H2AX in epithelioid histiocytes, inflammatory cells and enterocytes (arrowheads), B; Expression of γ-H2AX in villus epithelium and inflammatory cells (arrowheads), IHC, 20×. C; Expression of γ-H2AX (arrowheads) in inflammatory cells in the mesenterial lymph node, IHC, 20×. D; 8-Ohdg expression in epithelioid histiocytes, inflammatory cells and enterocytes (arrowheads), IHC, 20×. E; 8-Ohdg expression (arrowheads) in villi epithelium and inflammatory cells, IHC, 20×. F; 8-Ohdg expression (arrowheads) in inflammatory cells in the mesenterial lymph node, IHC, 20×

The macroscopic alterations discerned during necropsies of MAP-afflicted animals provide valuable diagnostic insights, distinguishing it from other gastrointestinal maladies. Notably, while most intestinal infections in ruminants typically manifest as erosive-ulcerative or exudative, MAP infections are hallmarked by proliferative inflammation within the tissues [15, 16]. Such inflammation predominantly exhibits macroscopic tissue thickening, a feature also observed in this study, especially in the mucosal thickening and folding of the intestines. Concurrently, the disease impacts the mesenterial lymph nodes and lymphatic vessels. While certain studies have highlighted frequent occurrences of caseous necrosis within mesenterial lymph nodes, others reported its rarity [17, 18].

In the made research, such necrotic clusters were infrequently identified. Lymphatic vessel thickening stands out as a recurrent macroscopic observation in MAP infections. It's theorized that obstructions arising from lymphangitis may play a pivotal role in the accumulation of fluid within the abdominal cavity. Furthermore, the pronounced oedema witnessed in both the abdominal region and beneath the chin can primarily be attributed to acute hypoproteinemia, a consequence of malabsorption due to extensive intestinal mucosal damage. Interestingly, despite the glaring hypoproteinemia, the incidence of dehydration-induced mortality remains relatively low, potentially owing to the duodenum's minimal damage, which is responsible for absorbing a significant portion of the stomach's fluid content. Consequently, fatalities due to acute dehydration are infrequent. Although affected animals maintain regular appetite levels, they exhibit cachexia and oedema stemming from hypoproteinemia. malabsorption, in turn, culminates in serous fat atrophy resulting from energy deficits [15, 16, 17]. Corroborating prior research, this study identified lymphadenitis, lymphangitis, ascites, cachexia, and serous fat atrophy in affected subjects.

During chronic infections, there is typically an influx of lymphoplasmacytic cells and fibroblasts at the inflammation site. In the case of chronic MAP infection, the predominant inflammatory cell infiltration is primarily composed of mononuclear leukocytes. The hallmark microscopic manifestation of MAP infection is the aggregation of epithelioid macrophages. These inflammatory responses are primarily located within the villous lamina propria and submucosa, accompanied by vascular alterations. Concurrently, along with proliferative characteristics, lesions indicative of tissue destruction is also evident. It's recognized that inflammatory modifications are predominantly found in the small intestine's distal portion [8, 19, 20].

This localized prevalence is believed to arise because the causative agents predominantly are captured by M cells in this region to breach the submucosa. When examining MAP infection through numerous studies, its histopathological presentation can generally be categorized into two distinct forms. The first is the paucibacillary form, characterized by a lymphocyte predominance and associated with a Th-1 cell-mediated immune response. In contrast, the multibacillary form is dominated by epithelioid macrophages and correlates with a Th-2 humoral immune response. Both experimental and naturally occurring infection studies have consistently reported the multibacillary form as the more prevalent [2, 21, 22].

Similar to the infiltration patterns seen in the intestinal submucosa, mesenterial lymph nodes also exhibit lymphoplasmacytic and macrophage infiltrations. However, the inflammation's intensity in the lymph nodes has been described variably across studies, with some reporting severe manifestations and others indicating milder presentations [18, 23]. In the present investigation, the observed patterns aligned with those from prior research. Additionally, it was ascertained that the multibacillary form was present in almost all studied animals, with lesions in the lymph nodes appearing less severe.

Cellular damage underpins the majority of diseases, and there's a prevailing theory that pathogens may directly or indirectly inflict DNA damage, especially in the case of infections [24, 25]. While various studies have delved into the pathogenesis of MAP infection, the complete understanding of its pathogenesis remains elusive. In an attempt to elucidate this, past research on MAP infections in cattle, sheep, goats, and camels primarily focused on proinflammatory cytokines, acute phase proteins, and oxidative stress parameters [23, 26, 27]. Yet, there seems to be a gap in the literature regarding DNA damage assessment in MAP infection.

In the present study, showcased the expression of γ-H2AX, a biomarker indicative of double-stranded DNA breaks, in the case of MAP infection. There is limited research utilizing γ-H2AX as a biomarker in animals. For instance, Nakamura *et al.* [28] applied this biomarker to identify DNA breaks in bovine lymphocytes post the Fukushima disaster. Toyoda *et al.* [29] highlighted the DNA damage in genotoxic urinary bladder cancers using γ-H2AX expression. Both Fradet-Turcotte *et al.* [30] and Sakakibara *et al.* [31] postulated that papilloma viruses induce DNA damage as evidenced by γ-H2AX expression. Drawing parallels with previous studies, in the this research underscores that MAP indeed induces DNA breaks in affected tissues, as evidenced by γ-H2AX expression.

Infection-induced tissue damage triggers inflammation, subsequently activating phagocytic cells. This activation gives rise to the production of free radicals. These reactive oxygen species amplify the extent of tissue damage. In the case of MAP infection, oxidative stress markers such as Superoxide Dismutase (SOD), Malondialdehyde (MDA), Glutathione (GSH), Nitric Oxide (NO), and Thiobarbituric Acid Reactive Substances (TBARS) have been examined across various animal species [23, 27, 32]. Yet, research pinpointing DNA oxidation in MAP infection remains absent. The modern biomarker, 8-Ohdg, has been employed to elucidate DNA oxidation in certain animal species and varied diseases. For example, Karakurt *et al.* highlighted DNA damage in ovine pulmonary adenocarcinoma using 8-Ohdg [33]. In a separate study, Karakurt underscored DNA oxidation in bovine papilloma and fibropapilloma via 8-Ohdg expression [34]. In the made study, the occurrence of DNA oxidation in the case of MAP infection was depicted through 8-Ohdg expression.

CONCLUSION

To effectively combat any disease and establish an impactful treatment regimen, a thorough understanding of its pathogenesis is imperative. Given the significance of MAP infection, perceived as a global threat affecting both animal and human health and resulting in economic loss, this study illuminates that the causative agent induces DNA breaks and oxidation in infected tissues. In made been this research has pioneered the elucidation of the DNA damage mechanism in MAP infection, marking a significant contribution to the global scientific community. In addition, this is the first study reported in the world to show the expression of γ-H2AX, a current DNA damage marker, and 8-Ohdg, an important DNA oxidation biomarker, in natural infection of Mycobacterium avium subspecies paratuberculosis in goats.

Conflict of interests

No conflicts of interest for all authors are declared.

BIBLIOGRAPHIC REFERENCES

[1] Idris SM, Eltom KH, Okuni JB, Ojok L, Elmagzoub WA, El Wahed AA, Eltayeb ES, Gameel AA. Paratuberculosis: The hidden killer of small ruminants. Animals. [Internet]. 2021; 12(1):12. doi: https://doi.org/grhbk3

[2] Verin R, Perroni M, Rossi G, De Grossi L, Botta R, De Sanctis B, Rocca S, Cubeddu T, Crosby-Durrani H, Taccini E. Paratuberculosis in sheep: Histochemical, immunohistochemical and *in situ* hybridization evidence of in utero and milk transmission. Res. Vet. Sci. [Internet]. 2016; 106(2016):173–179. doi: https://doi.org/f8rkt8

[3] Roller M, Hansen S, Knauf-Witzens T, Oelemann WMR, Czerny CP, Abd El Wahed A, Goethe R. *Mycobacterium avium* subspecies *paratuberculosis* infection in Zoo animals: A review of susceptibility and disease process. Front. Vet. Sci. [Internet]. 2020; 7:572724. doi: https://doi.org/m4pz

[4] Roberto JPdL, Limeira CH, Barnabé NNdC, Soares RR, Silva MLCR, Gomes AAdB, Higino SSdS, de Azevedo SS, Alves CJ. Antibody detection and molecular analysis for *Mycobacterium avium* subspecies *paratuberculosis* (MAP) in goat milk: Systematic review and meta-analysis. Res. Vet. Sci. [Internet]. 2021; 135:72–77. doi: https://doi.org/m4p2

[5] Mikkelsen H, Aagaard C, Nielsen SS, Jungersen G. Review of *Mycobacterium avium* subsp. *paratuberculosis* antigen candidates with diagnostic potential. Vet. Microbiol. [Internet]. 2011; 152(1–2):1–20. doi: https://doi.org/dckknv

[6] Sweeney RW. Pathogenesis of paratuberculosis. Vet. Clin. North Am. Food Anim. Pract. [Internet]. 2011; 27(3):537–546. doi: https://doi.org/ct2bgc

[7] Dennis MM, Reddacliff LA, Whittington RJ. Longitudinal study of clinicopathological features of Johne's disease in sheep naturally exposed to *Mycobacterium avium* subspecies paratuberculosis. Vet. Pathol. [Internet]. 2011; 48(3):565–575. doi: https://doi.org/c3rdj4

[8] Collins MT. Diagnosis of paratuberculosis. Vet. Clin. North Am. Food Anim. Pract. [Internet]. 2011; 27(3):581–591. doi: https://doi.org/bxzvsw

[9] Lawrence J, Karpuzoglu E, Vance A, Vandenplas M, Saba C, Turek M, Gogal Jr RM. Changes in γ-H2AX expression in irradiated feline sarcoma cells: an indicator of double strand DNA breaks. Res. Vet. Sci. [Internet]. 2013; 94(3):545–548. doi: https://doi.org/f4w26t

[10] Waterman DP, Haber JE, Smolka MB. Checkpoint responses to DNA double-strand breaks. Annu. Rev. Biochem. [Internet]. 2020; 89:103–133. doi: https://doi.org/ghqjkx

[11] Omari Shekaftik S, Nasirzadeh N. 8-Hydroxy-2' -deoxyguanosine (8-OHdG) as a biomarker of oxidative DNA damage induced by occupational exposure to nanomaterials: A systematic review. Nanotoxicology. [Internet]. 2021; 15(6):850–864. doi: https://doi.org/m4p5

[12] AbuArrah M, Setianto BY, Faisal A, Sadewa AH. 8-Hydroxy-2-deoxyguanosine as oxidative DNA damage biomarker of medical ionizing radiation: A scoping review. J. Biomed. Phys. Eng. [Internet]. 2021; 11(3):389-402. doi: https://doi.org/gj8vzw

[13] Dörtbudak M, Sağlam Y, Yıldırım S, Timurkan M. Examen de adenovirus con métodos moleculares y patológicos en casos de pneumonía ovina. Rev. MVZ Córdoba. [Internet]. 2022; 27(Supl):e2738. doi: https://doi.org/mqsc

[14] Kravitz A, Pelzer K, Sriranganathan N. The paratuberculosis paradigm examined: a review of host genetic resistance and innate immune fitness in *Mycobacterium avium* subsp. *paratuberculosis* infection. Front. Vet. Sci. [Internet]. 2021; 8:721706. doi: https://doi.org/m4p8

[15] Krüger C, Köhler H, Liebler-Tenorio EM. Cellular composition of granulomatous lesions in gut-associated lymphoid tissues of goats during the first year after experimental infection with *Mycobacterium avium* subsp. *paratuberculosis*. Vet. Immunol. Immunopathol. [Internet]. 2015; 163(1-2):33-45. doi: https://doi.org/m4p9

[16] Khodakaram Tafti A, Rashidi K. The pathology of goat paratuberculosis: Gross and histopathological lesions in the intestines and mesenteric lymph nodes. J. Vet. Med. B. [Internet]. 2000; 47(7):487-495. doi: https://doi.org/cgqvr9

[17] Hailat NQ, Hananeh W, Metekia AS, Stabel JR, Al-Majali A, Lafi S. Pathology of subclinical paratuberculosis (Johne's Disease) in Awassi sheep with reference to its occurrence in Jordan. Vet. Med. – Czech [Internet]. 2010; 55(12):590-602. doi: https://doi.org/m4qb

[18] Kheirandish R, Sami M, Khalili M, Shafaei K, Azizi S. Diagnosis of paratuberculosis in fresh and paraffin embedded samples by histopathology, PCR and immunohistochemistry techniques. Bulg. J. Vet. Med. [Internet]. 2017; 20(4):339-347. doi: https://doi.org/m4qc

[19] Derakhshandeh A, Namazi F, Khatamsaz E, Eraghi V, Hemati Z. Goat paratuberculosis in Shiraz: Histopathological and molecular approaches. Vet. Res. Forum. [Internet]. 2018; 9(3):253-257. doi: https://doi.org/m4qd

[20] Zarei-Kordshouli F, Geramizadeh B, Khodakaram-Tafti A. Prevalence of *Mycobacterium avium* subspecies *paratuberculosis* IS 900 DNA in biopsy tissues from patients with Crohn's disease: histopathological and molecular comparison with Johne's disease in Fars province of Iran. BMC Infect. Dis. [Internet]. 2019; 19(23):1-11. doi: https://doi.org/m4qf

[21] Hemida H, Kihal M. Detection of paratuberculosis using histopathology, immunohistochemistry, and ELISA in West Algeria. Comp. Clin. Pathol. [Internet]. 2015; 24:1621-1629. doi: https://doi.org/m4qg

[22] Smeed JA, Watkins CA, Rhind SM, Hopkins J. Differential cytokine gene expression profiles in the three pathological forms of sheep paratuberculosis. BMC Vet. Res. [Internet]. 2007; 3(18):1-11. doi: https://doi.org/dsfjx5

[23] Sonawane GG, Tripathi BN. Expression of inflammatory cytokine and inducible nitric oxide synthase genes in the small intestine and mesenteric lymph node tissues of pauci-and multibacillary sheep naturally infected with *Mycobacterium avium* ssp. *paratuberculosis*. Int. J. Mycobacteriol. [Internet]. 2016; 5(Suppl. 1):S77-S78. doi: https://doi.org/m4qh

[24] Souliotis VL, Vlachogiannis NI, Pappa M, Argyriou A, Ntouros PA, Sfikakis PP. DNA damage response and oxidative stress in systemic autoimmunity. Int. J. Mol. Sci. [Internet]. 2019; 21(1):55. doi: https://doi.org/m4qj

[25] Kumar N, Raja S, Van Houten B. The involvement of nucleotide excision repair proteins in the removal of oxidative DNA damage. Nucleic Acids Res. [Internet]. 2020; 48(20):11227-11243. doi: https://doi.org/m4qk

[26] Bozukluhan K, Merhan O, Büyük F, Akyüz E, Gezer T, Eğritağ HE, Gökçe G. [Determination of Some Acute Phase Protein and Biochemical Parameter Levels in Cattle Infected with *Mycobacterium avium* subsp. *paratuberculosis*]. Bozok Vet. Sci. [Internet]. 2022 [cited 26 Oct. 2023]; 3(2):47-51. Turkish. Available in: https://goo.su/5zZVXrl

[27] El-Deeb WM, Fouda TA, El-Bahr SM. Clinico-biochemical Investigation of Paratuberculosis of Dromedary Camels in Saudi Arabia: Proinflammatory Cytokines, Acute Phase Proteins and Oxidative Stress Biomarkers. Pak. Vet. J. [Internet]. 2014 [cited 18 Oct. 2023]; 34(4):484-488. Available in: https://goo.su/BaJnpB

[28] Nakamura AJ, Suzuki M, Redon CE, Kuwahara Y, Yamashiro H, Abe Y, Takahashi S, Fukuda T, Isogai E, Bonner WM. Fukumoto M. The causal relationship between DNA damage induction in bovine lymphocytes and the Fukushima nuclear power plant accident. Radiat. Res. [Internet]. 2017; 187(5):630-636. doi: https://doi.org/f9sxc9

[29] Toyoda T, Cho YM, Akagi JI, Mizuta Y, Hirata T, Nishikawa A, Ogawa K. Early detection of genotoxic urinary bladder carcinogens by immunohistochemistry for γ-H2AX. Toxicol. Sci. [Internet]. 2015; 148(2):400-408. doi: https://doi.org/f74t2c

[30] Fradet-Turcotte A, Bergeron-Labrecque F, Moody CA, Lehoux M, Laimins LA, Archambault J. Nuclear accumulation of the papillomavirus E1 helicase blocks S-phase progression and triggers an ATM-dependent DNA damage response. J. Virol. [Internet]. 2011; 85(17):8996-9012. doi: https://doi.org/c3hrxd

[31] Sakakibara N, Mitra R, McBride AA. The papillomavirus E1 helicase activates a cellular DNA damage response in viral replication foci. J. Virol. [Internet]. 2011; 85(17):8981-8995. doi: https://doi.org/cjgd8b

[32] Espinosa J, de la Morena R, Benavides J, García-Pariente C, Fernández M, Tesouro M, Arteche N, Vallejo R, Ferreras MC, Pérez V. Assessment of acute-phase protein response associated with the different pathological forms of bovine paratuberculosis. Animals. [Internet]. 2020; 10(10):1925. doi: https://doi.org/m4qm

[33] Karakurt E, Beytut E, Dağ S, Nuhoğlu H, Yıldız A, Kurtbaş E. Assessment of MDA and 8-OHdG expressions in ovine pulmonary adenocarcinomas by immunohistochemical and immunofluorescence methods. Acta Vet. Brno. [Internet]. 2022; 91(3):235-241. doi: https://doi.org/m4qn

[34] Karakurt E. Immunohistochemical Investigation of Oxidative Stress-induced DNA Damage and Lipid Peroxidation in Bovine Papillomas and Fibropapillomas. Van Vet J. [Internet]. 2021; 32(1):22-27. doi: https://doi.org/m4qp